The Effects of Transient Overvoltages on the Reliability of HVDC Extruded Cables. Part 2: Superimposed Switching Impulses

The Effects of Transient Overvoltages on the Reliability of HVDC Extruded Cables. Part 2: Superimposed Switching Impulses

Giovanni Mazzanti, *Fellow, IEEE*, Bassel Diban, *Member, IEEE*

***Abstract*-- In a previous paper (Part 1) the authors have performed the simulative evaluation of the life lost by HVDC extruded cables subjected to long TOVs occurring in VSC HVDC cable systems. The conclusions were that it cannot be completely ruled out that the field levels and the duration of such TOVs are a potential threat to certain cable designs, and tests other than Load Cycling Type Tests after CIGRÉ Technical Brochure 496 could assess quantitatively the potential threat associated with long TOVs. For these reasons, in this Part 2 superimposed switching impulses applied during Type Tests after TB 496 are analyzed in order to check if such impulses might be equivalent to long TOVs as for their electro-thermal stress effects on extruded insulation. The analysis is similar to that carried out for long TOVs in Part 1, i.e. it consists of: calculating the electric field during superimposed switching impulses; comparing it with the field during long TOVs; calculating with Miner's law of cumulated damage the life lost during superimposed switching impulses and comparing it with the loss of life during TOVs. A brief literature survey of potential high field effects during long TOVs is also reported.**

***Index Terms*-- Cross linked polyethylene insulation, HVDC insulation, Life estimation, Power cables, Reliability estimation, Switching transients, Surges.**

I. Introduction

With the advent of Voltage Source Converter (VSC) HVDC cable systems, several simulations have been carried out to calculate external and internal overvoltages superimposed onto DC voltage in such systems [1]-[8] and CIGRÉ Joint Working Group B4/B1/C4.73 has been also formed to study such over-voltages [3],[9] within Modular Multilevel Converter (MMC) HVDC transmission systems in different configurations (monopolar, rigid bipolar). Overall, these simulations have shown that severe long Temporary Over-voltages (TOVs) may arise: level, risetime and duration of overvoltage depend on fault location, loading of line, surge arrester characteristics, DC cable length, grounding methods, etc. One of the most severe situations, studied in [1],[2], occurs in case of pole-to-ground faults in symmetric monopolar VSC HVDC cable systems, yielding a maximum overvoltage in the middle of the healthy pole up to 1.8 p.u. of the pre-fault DC voltage or even higher, with voltage rise time ≈ few ms and overall duration ≈ one hundred ms or more until cable discharge. This long TOV, regarded and referred to here as "worst-case TOV", is sketched in Fig. 1 and the orders of magnitude of its parameters are listed in Table I.

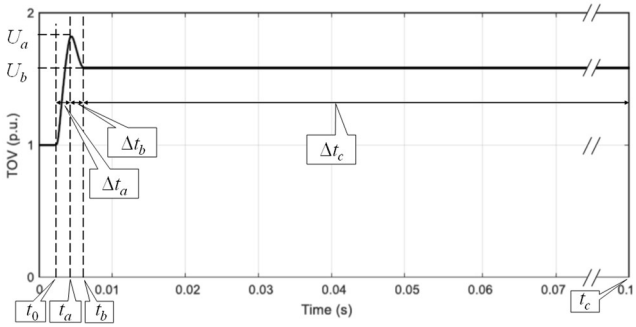

Fig. 1. Worst-case long TOV in VSC HVDC cable in symmetrical monopolar configuration (reprocessed from [3]).

TABLE I
ORDERS OF MAGNITUDE OF PARAMETERS OF WORST-CASE LONG TOV IN FIG. 1 (SYMMETRICAL MONOPOLAR CONFIGURATION)

parameter	name	value
U_a	peak voltage	≈1.8 (p.u. of rated voltage U_0)
U_b	plateau voltage	≈1.6 p.u. (p.u. of rated voltage U_0)
$\Delta t_a = t_a - t_0$	Time to Peak	≈5 ms
$\Delta t_b = t_b - t_a$	Time of peak decay	≈5 ms
$\Delta t_c = t_c - t_b$	Time of Plateau	≈100 ms

In previous Part 1 paper [10] the authors have performed the simulative evaluation of the life lost by HVDC extruded cables subjected to the worst-case TOV. The conclusions were that the maximum field during this TOV - occurring at inner insulation surface - is higher, in both Cold and Hot cable conditions, than the maximum field at inner insulation during the Load Cycling Type-Test (LCTT) after CIGRÉ Technical Brochure (TB) 496 [5], performed at a DC voltage U_T=1.85U_0. Hence, it cannot be completely ruled out that the field levels and the duration of such TOVs are a potential threat to certain cable design, and tests other than Type-Test load cycles could assess quantitatively the potential threat of long TOVs.

For these reasons, the present Part 2 paper aims at checking if superimposed switching impulses – those closest to long TOVs among the waveshapes applied during Electrical Type Tests after TB 496 [11] – can have an effect "equivalent" to long TOVs, in the sense that they can be at least as challenging as the TOV in terms of electric and thermal stresses applied to the tested HVDC cable system. A preliminary check is done by

G. Mazzanti and B. Diban are with the Dept. of Electrical, Electronic and Information Engineering "Guglielmo Marconi", University of Bologna, Viale Risorgimento 2, 40136 Bologna, Italy (e-mail: giovanni.mazzanti@unibo.it).

evaluating the total electric field within cable insulation thickness during the superimposed switching impulses after [11] (calculated as the superposition of a DC steady-state field plus an impulsive AC field), and then comparing it for the cable in both cold and hot conditions with the electric field during the long TOV. Thereafter Miner's law of cumulated damage is used to assess the effect of cumulated aging during the superimposed switching impulses on the loss of life of the various points within cable insulation, thereby completing quantitatively the severity assessment of the superimposed switching impulses. An overall comparison of TOVs vs. superimposed switching impulses and a brief literature survey of possible high field effects during long TOVs close the paper.

II. Field and Loss-of-Life Estimation under the Superimposed Switching Impulse of Same Polarity

A. Why Superimposed Switching Impulse of Same Polarity

First of all, let us clarify that the first goal here is finding a voltage waveshape – among those applied in existing test procedures for HVDC extruded cables – which is potentially equivalent to the long TOV of Fig. 1 from the viewpoint of the effect on extruded insulation for HVDC VSC cables. Actually, the main standards for testing HVDC extruded cable systems are CIGRÉ TB 496 [11] and IEC Standard 62895 [12], and the only transient voltage waveshapes superimposed onto DC voltage found in [5],[12] are superimposed switching and superimposed lightning impulses. Between these two, here superimposed switching impulses are considered as the waveshapes potentially equivalent to the long TOV of Fig. 1 from the viewpoint of their effect on HVDC extruded cables. Indeed, although both lightning and switching superimposed impulses feature - as the long TOV - a transient fast-varying voltage superimposed onto the rated DC voltage, the standard switching impulse lasts much longer than the standard lightning impulse [13], which makes it much closer to the long TOV as for its duration. This notwithstanding the front time of the overvoltage (depending on cable length) can be in the range of 5-10 ms for long cable schemes [1]-[9], hence much longer than the rise time of the standard switching impulse (250 μs).

In detail, comparing the standard switching impulse with the time intervals Δt_a, Δt_b, Δt_c of the TOV in Fig. 1 it stems that:

- the front duration T_1=250 μs=0.25 ms of the standard switching impulse could be associated with the "front duration" or rising voltage time interval Δt_a of the TOV, since during both T_1 and Δt_a the voltage rises fast;
- the time-to-half value T_2=2500 μs=2.5 ms of the standard switching impulse could be associated with the overall time interval $\Delta t_b+\Delta t_c$ of the TOV, since during both T_2 and $\Delta t_b+\Delta t_c$ the applied voltage drops at a much milder pace - it is even steady during Δt_c.

However, on the whole even the switching impulse is much shorter – 20÷40 times – that the long TOV, since it holds:

$$T_1 = 0.25 \text{ ms} << \Delta t_a = 5 \text{ ms} \quad (1)$$

$$T_2 = 2.5 \text{ ms} << \Delta t_b+\Delta t_c = 5 \text{ ms} + 100 \text{ ms} = 105 \text{ ms} \quad (2)$$

Hence it can be said qualitatively[1] that the Superimposed Switching Impulse Voltage Test (SSIVT) after [11] can encompass the worst-case TOV of Fig. 1 – making in principle dedicated tests for long TOVs not needed – only provided that:

1) the maximum voltage/electric field during the SSIVT at the most severely stressed location within cable insulation is much higher than the maximum voltage/electric field during the TOV, so as to compensate for the much shorter duration of the switching impulse compared to the TOV;
2) the most stressed location during the SSIVT is the same as during the TOV, namely inner insulation;
3) the polarity of the impulse during the SSIVT is the same as that of rated DC voltage U_0, like during the TOV.

Requirement 3) can be easily matched by discarding – among the superimposed impulse voltages prescribed by [11] for VSC HVDC extruded cables – Superimposed Switching Impulses of the Opposite Polarity to rated DC voltage (SSIOP) and considering only Superimposed Switching Impulses of the Same Polarity (SSISP) as the rated DC voltage. The matching of above requirements 1) and 2) can only be assessed via calculations, once the peak value $U_{P2,S}$ of SSISP has been fixed.

To fix such value, let us recall that in [11] $U_{P2,S}$ is defined as 1.15 × the maximum absolute peak value of the switching impulse voltage which the cable system can experience when the impulse has the same polarity as U_0. Then, from requirement 1) above and considering that the maximum field during the TOV is higher than the maximum field at inner insulation during the LCTT performed at U_T=1.85 U_0 [10], it can be agreed that a meaningful lower bound of the prospective range of values of $U_{P2,S}$ to analyze is as follows:

$$U_{P2,S,min} = 1.15 \times U_T = 1.15 \times 1.85\ U_0 = 2.1275 \approx 2.15 \quad (3)$$

As for the upper value, $U_{P2,S,max}$, many different choices can be done also considering the switching impulse voltage withstand levels of existing HVDC extruded cable projects. For the sake of an exhaustive parametric analysis, let us double the 15% safety margin used for $U_{P2,S,min}$ and choose $U_{P2,S,max}$ as:

$$U_{P2,S,max} = 1.30 \times U_T = 1.30 \times 1.85\ U_0 = 2.405 \approx 2.4 \quad (4)$$

B. Calculation of the Electric Field during the SSISP

As a premise to computing the field during the SSISP, it must be observed that the overall duration of the SSISP is T_S≈5 ms, as deduced from Fig. 2 (reprocessed from Figure 14 after [13]). Indeed, the time-to-half value T_2 actually includes the front duration T_1: hence, the total duration of the tail of the switching impulse, T_{tail}, and the total duration of the whole switching impulse, T_S, are respectively equal to:

$$T_{tail} = 2\times(T_2 - T_1) = 2\times(2.5 - 0.25) \text{ ms} = 4.5 \text{ ms} \quad (5)$$

$$T_S = T_1 + T_{tail} = 0.25 + 4.5 \text{ ms} = 4.75 \text{ ms} \approx 5 \text{ ms} \quad (6)$$

Thus the overall duration of the SSISP, T_S≈5 ms, is

[1] A more quantitative statement is trialed later on in Section III.C.

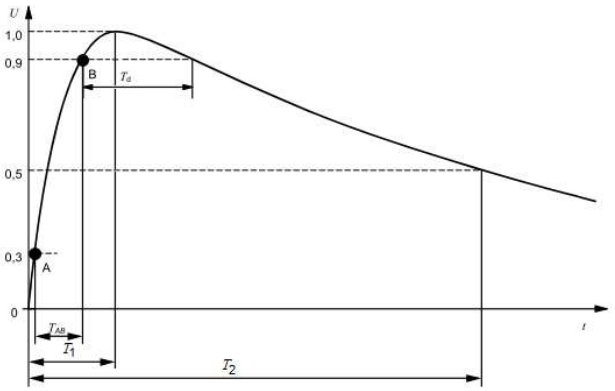

Fig. 2. Schematic of the switching impulse voltage. After IEC 60060-1 [13].

dramatically shorter than the dielectric time constant $\tau=\varepsilon/\sigma$ (where ε and σ are, respectively, permittivity and electrical conductivity) and the time for stability 10 τ (i.e. the time to the attainment of the steady state distribution of electric field) of dielectrics used for DC extruded cables [10],[11]. This situation was already shown in [10] for the worst-case TOV with reference to both Cold Cable conditions (i.e. cable at zero load) and Hot Cable conditions (i.e. cable at full load), but it holds a fortiori for the much shorter SSISP. This can be summarized as:

$$T_S \approx 5 \text{ ms} << T_{TOV} \approx 110 \text{ ms} << \tau << 10\ \tau \tag{7}$$

Thus, as established in [10] for the long TOV, a fortiori the SSISP does not perturb the pre-existing resistive electric field due to rated DC voltage U_0; such resistive field can be assumed to have already reached steady state for the purpose of evaluating the total electric field during the SSISP. Hence, for a homogeneous insulation the total electric field $E_{SSISP}(r,t)$ at a radial coordinate r within cable insulation and at a time t during a SSISP - of duration T_S, transient voltage $U_p(t)$ and resulting peak voltage U_P - superimposed onto rated DC voltage U_0, can be calculated essentially in the same way as for the worst-case TOV in [10], namely as the superposition of [14],[15]:

- $E_{DC,U0}(r)$, the resistive steady-state DC field due to U_0;
- $E_p(r,t)$, the capacitive AC field due to the SSISP $U_p(t)$ as it exceeds U_0 within time intervals T_1 and T_2:

$$E_{SSISP}(r,t)=E_{DC,U0}(r)+E_p(r,t) \tag{8}$$

As shown in [10], for practical and preliminary evaluation purposes $E_{DC,U0}(r)$ can be well approximated by the following Eoll's formula [10],[15]:

$$E_{DC,U0}(r) = \delta U_0 \left(\frac{r}{r_o}\right)^{\delta-1} / \left\{ r_o \left[1-\left(\frac{r_i}{r_o}\right)^{\delta}\right]\right\} \tag{9}$$

$$\delta = \left[\frac{a\Delta T}{ln(r_o/r_i)} + \frac{bU_{DC}}{(r_o-r_i)}\right] / \left[1+\frac{bU_{DC}}{(r_o-r_i)}\right] \tag{10}$$

where:

- r_i = inner radius of cable insulation;
- r_o = outer radius of cable insulation;
- $r\in[r_i,r_o]$ = radial coordinate within cable insulation;
- ΔT = temperature drop across insulation thickness;
- W_C = conductor losses per unit of length;
- a = temperature coefficient of electrical conductivity;
- b = electric field coefficient of electrical conductivity.

As explained in [14],[15], $E_p(r,t)$ in (8) can be written as follows - recalling that the impulse voltage $U_p(t)$ during the SSISP has the same polarity as U_0:

$$E_p(r,t) = \frac{U_p(t)-U_0}{r\ ln(r_o/r_i)} \tag{11}$$

After the above considerations, a preliminary evaluation of the severity of the electric field during the SSISP for an HVDC extruded cable is carried out in the following steps.

1) Choice of a typical case-study cable.
2) Calculation for this cable in
   i) Cold Cable conditions, i.e. zero load current;
   ii) Hot Cable conditions, i.e. full load current;
   of the following quantities:
   a) temperature profiles $T(r)$;
   b) DC field $E_{DC,U0}(r)$ at voltage $U_{DC}=U_0$ via (9);
   c) AC field $E_p(r)$ during the SSISP via (11);
   d) total field $E_{SSISP}(r,t)$ via (8);
3) Comparison of $E_{SSISP}(r,t)$ with $E_{TOV}(r,t)$ to assess if the SSISP field can encompass the long TOV field.

Calculations at above point 2b) - already reported in Part 1 [10] and omitted here for brevity - rely on three different sets of conductivity coefficients a, b of the insulation:

I) the "low set", a_L=0.042 K^{-1}, b_L=0.032 mm/kV;
II) the medium set, a_M=0.084 K^{-1},b_M=0.0645 mm/kV;
III) the "high set", a_H=0.101 K^{-1}, b_H=0.0775 mm/kV.

The low set a_L,b_L, the medium set a_M, b_M and the high set a_H,b_H fall, respectively, at the lower bound, in the middle and at the upper bound of the typical range of variation of conductivity coefficients for DC-XLPE compounds [16]-[19].

C. Estimation of Life Fraction Lost during the SSISP

A more quantitative assessment of the severity of the SSISP for the extruded insulation of HVDC cables can be achieved by evaluating the aging effects cumulated during the SSISP in terms of life lost at the various points within cable insulation thickness. This can be done resorting to Miner's law of cumulated damage/aging [20], applied for the life estimation of HVAC cables [21],[22] and later on also of HVDC cables [17]-[19] in the presence of time-varying electro-thermal stress. In summary, Miner's law is based on the observation that in HV cables subjected to time-varying electro-thermal stress - e.g. due to load cycles as in [17]-[19],[21],[22], or due to the time variation of applied voltage as in the presence of the SSISP (or of long TOV as in [10]) - the cable can be assumed to fail as its insulation fails because of the electro-thermal aging cumulated at the most severely stressed point $r^*\in[r_i,r_o]$ within cable insulation. This aging can be estimated by evaluating the "infinitesimal loss-of-life fraction" $dLF(r^*,t)$ relevant to each infinitesimal interval dt between t and $t+dt$ wherein electro-thermal stress (absolute temperature $T(r^*,t)$ and electric field $E(r^*,t)$) can be deemed as constant:

$$dLF(r*,t) = dt/L[E(r*,t),T(r*,t)] \tag{12}$$

where $L[E(r^*,t),T(r^*,t)]$ is life at electric field $E(r^*,t)$ and temperature $T(r^*,t)$. This life can be estimated resorting to a proper life model for cable insulation subjected to constant values of temperature $T(r^*,t)$ and electric field $E(r^*,t)$.

Therefore, in order to determine the "total loss-of-life fraction" $\Delta LF(r^*)$ relevant to the total time period Δt_P where stress varies according to a known time pattern, e.g.:

- the time pattern of the TOV of Fig. 1, as in [10];
- the time pattern of the SSISP, as in the present paper;

the infinitesimal loss-of-life fractions $dLF(r^*,t)$ have to be integrated over Δt_P, as follows:

$$\Delta LF(r^*) = \int_{\Delta t_P} dLF(r^*) = \int_{\Delta t_P} \frac{dt}{L[E(r^*,t),T(r^*,t)]} \qquad (13)$$

Now, the calculation of the total loss-of-life fraction $\Delta LF_{SSIP}(r^*)$ according to (13) requires that a proper life model for cable insulation subjected to constant values of electric field $E(r^*,t)$ and temperature $T(r^*,t)$ is found, namely a proper function $L=f[E(r^*),T(r^*)]$ expressing the relationship between cable insulation life L and stresses $T(r^*)$ and $E(r^*)$. Since during the SSISP, which lasts around 100 ms, cable temperature can be reasonably assumed as constant when considering the thermal time constant of HV cables [23], the life model for cable insulation can be focused on the dependence of cable life on electric field $E(r^*)$ only, namely on function $L=f[E(r^*)]$. To find this function, first the Inverse Power Model (IPM) after TB 496 can be taken for the relationship between voltage and time-to-failure, which can be recast as follows [10], [11],[15]:

$$L = L_0 (U_0/U)^n \qquad (14)$$

where:

U = applied voltage;

L = time to failure at constant applied voltage U;

L_0 = design life (40 years for HVDC extr.cables [10], [11]);

n =life exponent (=10 for HVDC extruded cables [10],[11]).

As shown in [15], relationship (14) can be extended to electric field (stress) at the most stressed point within cable insulation, $E(r^*)$, thereby attaining the searched function $L=f[E(r^*)]$ as follows:

$$L = L_0 (E_0/E(r^*))^n \qquad (15)$$

where E_0 is the reference design field at the most stressed point within cable insulation in the reference design conditions of the cable (see [10] for more details).

III. Case Study

A. Case Study Cable

In this applicative section, for the sake of comparing the SSISP with the worst-case TOV let us focus on the same typical case-study cable already treated in [10] (similar results are obtained for other cable types, differing as for rated voltage, ampacity, etc.). It is a land XLPE-insulated HVDC cable for use with VSC, with the following main design parameters: U_0=320 kV, conductor cross section S=1,600 mm^2 (copper), DC-XLPE insulation with thickness s≈18 mm, rated current (ampacity) I_D=1,727 A, and rated conductor temperature θ_D = 70°C. Other design parameters are listed in Table II [17],[18].

TABLE II
Case-study Cable Characteristics

Parameter	Value
Rated power (bipolar scheme) [MW]	1,105
Rated voltage [kV]	320
Conductor Material	Cu
Insulation Material	DC-XLPE
relative permittivity ε_r	2.3
Rated conductor temperature θ_D [°C]	70
Ambient temperature θ_a [°C]	20
Conductor cross-section [mm^2]	1600
inner insulation radius r_i [mm]	24.6
Insulation thickness [mm]	17.9
outer insulation radius r_o [mm]	42.5
Design life L_D [years]	40
Design failure probability P_D [%]	1
Rated current [A]	1,727

B. Temperature Profiles for the Hot and Cold Cable Condition

For the case-study cable, the transient temperature profiles during one 24-hour load cycle for prequalification tests (PQT) and type tests (TT) according to [11] are reported in Fig. 2 of [10], omitted here for brevity. As observed in [10], the steady-state temperature reached within the insulation during the last 2 hours of the heating period of the 24-hour cycle can be taken as the Hot Cable Condition temperature profile, while the room temperature θ_a approximately reached at the end of the 16 h of the cooling period can be taken as the Cold Cable Condition uniform temperature profile within the insulation.

C. Field during the SSISP vs. Field during the TOV

The DC steady-state field profiles at rated voltage U_0=320 kV within the insulation of the case-study cable computed via (9) with the low set a_L,b_L and the high set a_H,b_H of temperature and field coefficients of conductivity for the Cold and Hot Cable temperature profiles are reported, respectively, in Fig. 3 (low set) and Fig. 4 (high set) of [10], together with the relevant DC LCTT electric field profiles at U_T=1.85U_0=592 kV. Figure 3 showed that for low set a_L,b_L the case-study cable does not exhibit field inversion as the load rises from zero to full, both at U_0 and at U_T, thus the maximum field stays at the inner insulation. On the contrary, Figure 4 showed that for high set a_H,b_H the case-study cable does exhibit field inversion as the load rises from zero to full, both at U_0 and at U_T, thus the maximum field moves from inner to outer insulation as the load current goes from 0 to cable ampacity.

Here, Figures 3 and 4 show the AC electric field $E_p(r,t)$ vs. time respectively during the front T_1 and the tail T_2 of the SSISP at 5 locations within the insulation of the case-study cable computed by means of (11) with $U(t)$ according to Fig. 2 and $U_P=U_{P2,S,min}$ =2.15 U_0. Figures 5 and 6 are the same as homologous Figs. 3 and 4, apart that $U_P=U_{P2,S,max}$=2.4 U_0, so as to scan the whole range of SSISP treated here. As obvious, AC field is higher when $U_P=U_{P2,S,max}$. For this reason all figures reporting total field hereafter are relevant to $U_P=U_{P2,S,max}$.

At this stage, total field can be calculated. For the low set

a_L,b_L Figure 7 displays the total electric field in the insulation wall of the Cold Cable vs. time during the whole SSISP with U_P=$U_{P2,S,max}$=2.4 U_0 at 5 locations within the insulation of the chosen cable, calculated through (8) as the superposition of DC field at U_0 for the Cold Cable (see Fig. 3 of [10]) plus the AC field during the whole SSISP with U_P=$U_{P2,S,max}$ plotted in Figs. 5, 6; Figure 8 is the same as Fig. 7, but for the Hot Cable.

Similarly, for the high set a_H,b_H Figure 9 reports the total electric field in the insulation wall of the Cold Cable vs. time during the whole SSISP with U_P=$U_{P2,S,max}$=2.4 U_0 at 5 locations within the insulation of the chosen cable, calculated through (8) as the superposition of DC field at U_0 for the Cold Cable (see Fig. 4 of [10]) plus the AC field during the whole SSISP with U_P=$U_{P2,S,max}$ plotted in Figs. 5, 6; Figure 10 is the same as Fig. 9, but for the Hot Cable.

Figures 7-10 emphasize that the maximum field during the SSISP always occurs at inner insulation due to the AC field, which is always maximum at inner insulation, see (11). Thus, inner insulation is always the most stressed point during the SSISP. This happens also during the worst-case TOV, thus this is another good reason for considering that SSISP can have an effect "equivalent" to long TOVs as for the electric field.

Table III shows a comprehensive comparison relevant to the low set of conductivity coefficients a_L,b_L, i.e. the highest total field due to the TOV within Δt_a, Δt_b, Δt_c at inner and outer insulation for the Hot and Cold Cable (calculated and reported in [10], Figs. 8, 9 and Table VI) vs. the highest field during the SSISP at inner and outer insulation for U_P=$U_{P2,S,min}$=2.15 U_0 and U_P=$U_{P2,S,max}$=2.4 U_0 (see Figs. 7,8). Similarly, Table IV shows a comprehensive comparison relevant to the high set of conductivity coefficients a_H,b_H, i.e. the highest total field due to the TOV within Δt_a, Δt_b, Δt_c at inner and outer insulation for the Hot and Cold Cable (calculated and reported in [10], Figs. 10, 11 and Table VII) vs. the highest field during the SSISP at inner and outer insulation for U_P=$U_{P2,S,min}$=2.15 U_0 and U_P=$U_{P2,S,max}$=2.4 U_0 (see Figs. 9,10). In Tables III, IV the cases when the TOV field exceeds the field during the LCTT after [5] are highlighted in light grey, to emphasize that these cases are, strictly speaking, not encompassed by the LCTT as for the field level applied during this test; the cases where the TOV field is exceeded by the field during the SSISP after [5] are highlighted in dark grey, to emphasize that these cases are, strictly speaking, encompassed by the SSISP as for the electric field level.

Table III shows that with the low set a_L,b_L:

- for the Cold Cable the maximum field during the TOV at inner insulation (40.6 kV/mm) is lower than the maximum field at inner insulation during the SSISP with both $U_{P2,S,min}$=2.15 U_0 (48.9 kV/mm, +17.0%) and $U_{P2,S,max}$=2.4 U_0 (54.8 kV/mm, +25.9%). The same holds for the field at outer insulation, although with a slightly lower margin;
- for the Hot Cable the maximum field during the TOV at inner insulation (37.1 kV/mm) is lower than the maximum field at inner insulation during the SSISP with both $U_{P2,S,min}$=2.15 U_0 (45.4 kV/mm, +18.3%) and $U_{P2,S,max}$=2.4 U_0 (51.4 kV/mm, +27.8%). The same holds also for the field at outer insulation, although with a lower margin.

Similarly, Table IV shows that with the high set a_H, b_H:

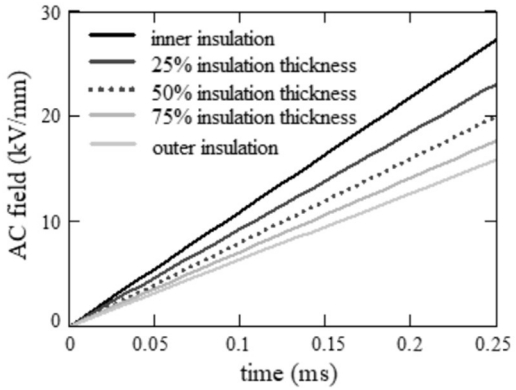

Fig. 3. AC electric field during the front T_1 of the SSISP vs. time at 5 locations within the insulation of the case-study cable. U_P=$U_{P2,S,min}$ =2.15 U_0

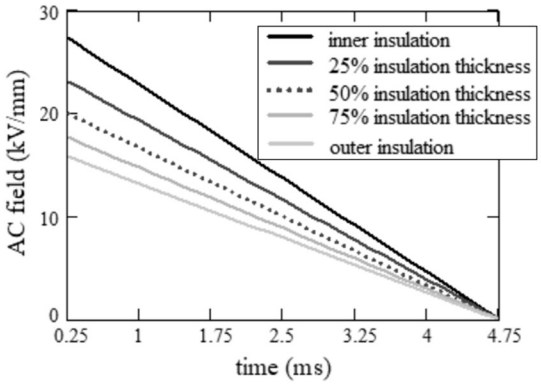

Fig. 4. AC electric field during the tail T_2 of the SSISP vs. time at 5 locations within the insulation of the case-study cable. U_P=$U_{P2,S,min}$=2.15 U_0

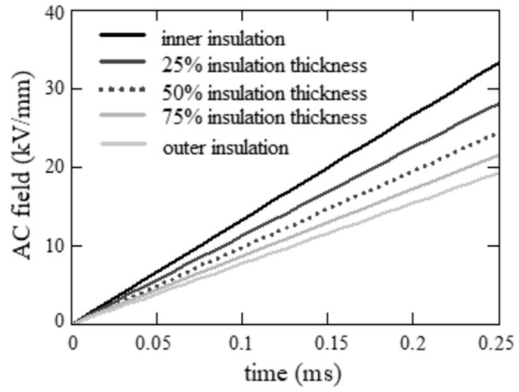

Fig. 5. AC electric field during the front T_1 of the SSISP vs. time at 5 locations within the insulation of the case-study cable. U_P=$U_{P2,S,max}$=2.4 U_0

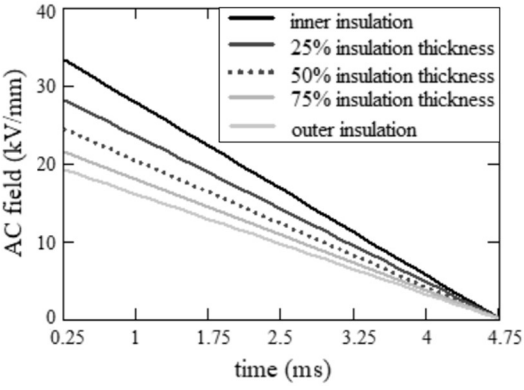

Fig. 6. AC electric field during the tail T_2 of the SSISP vs. time at 5 locations within the insulation of the case-study cable. U_P=$U_{P2,S,max}$=2.4 U_0

- for the Cold Cable the maximum field during the TOV at inner insulation (39.3 kV/mm) is lower than the maximum field at inner insulation during the SSISP with both $U_{P2,S,min}$=2.15 U_0 (47.6 kV/mm, +17.4%) and $U_{P2,S,max}$=2.4 U_0 (53.5 kV/mm, +26.5%). The same holds for the field at outer insulation, although with a slightly lower margin;
- for the Hot Cable the maximum field during the TOV at inner insulation (34.2 kV/mm) is lower than the maximum field at inner insulation during the SSISP with both $U_{P2,S,min}$=2.15 U_0 (42.6 kV/mm, +19.7%) and $U_{P2,S,max}$=2.4 U_0 (48.5 kV/mm, +29.5%). The same holds also for the field at outer insulation, although with a lower margin.

The similarity of the situation during the SSISP with the low set a_L,b_L and with the high set a_H, b_H is due to the fact that the AC field predominates more broadly during the SSISP than during the long TOV, because of the higher peak value of the former (2.15÷2.4U_0) with respect to the latter (1.8 U_0), and is confirmed by many simulations – omitted for brevity – done with other sets of a,b in-between a_L,b_L and a_H,b_H.

C. Results of Loss-of-Life Fraction Calculation during the SSISP and Comparison with the Long TOV

Table V lists the values of total loss-of-life fractions ΔLF at inner insulation – the most stressed point – calculated for the SSISP with a_L,b_L and a_H,b_H via (13), thus based on $E(r^*=r_i,t)$ with $t \in T_S$ from Figs. 7,9 for the Cold Cable, from Figs. 8,10 for the Hot Cable. The Table also shows the values of total loss-of-life fractions at inner insulation calculated for the long TOV in [10] and the percent difference Δ "TOV vs SSISP", i.e.:

$$\Delta=100\times[\Delta LF(\text{TOV}) - \Delta LF(\text{SSISP})]/\Delta LF(\text{SSISP}) \quad (16)$$

Table V proves that – as already found for the TOV in [10] - the life fraction lost during the SSISP at inner insulation is higher for the Cold than for the Hot Cable, since the field is higher for the Cold than for the Hot Cable (see Figs. 7, 9 vs. Figs. 8,10). The loss of life at inner insulation drops as a,b increase, since the maximum field at inner insulation also drops as a,b increase (compare Figs. 7,8 to Figs. 9,10, and Table III to Table IV), thus inner insulation is progressively less stressed.

IV. Discussion

The calculations reported in Tables III-IV outline that the maximum field during the SSISP – occurring at inner insulation – is significantly higher than the maximum field at inner insulation during the long TOV of Fig. 1 in both Cold and Hot Cable conditions, with all values of a,b ranging from the low set a_L,b_L to the high set a_H,b_H. The safety margin is already consistent with $U_{P2,S,min}$=2.15 U_0 (≈17-19%), but of course it is even broader with $U_{P2,S,max}$=2.4 U_0 (≈26-29%). The same holds also for the field at outer insulation, although with a lower margin. Thus, as for the electrothermal stress, the SSISP could in principle encompass the long TOV from the viewpoint of the stress intensity on the extruded insulation of HVDC cables.

On the other hand, the worst-case TOV lasts much longer than the SSISP, as made evident by the column "duration" in Tables III-IV, as well as by (1)-(2). Hence the overall aging

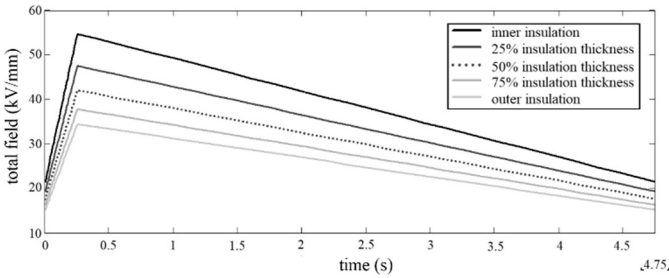

Fig. 7. Total electric field for the Cold Cable vs. time during the whole SSISP with $U_P=U_{P2,S,max}$=2.4 U_0 at 5 locations within the insulation. Low set a_L,b_L

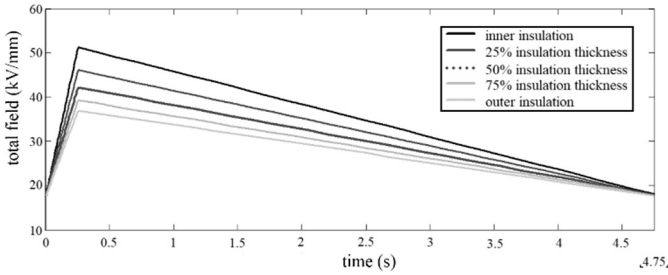

Fig. 8. Total electric field for the Hot Cable vs. time during the whole SSISP with $U_P=U_{P2,S,max}$=2.4 U_0 at 5 locations within the insulation. Low set a_L,b_L

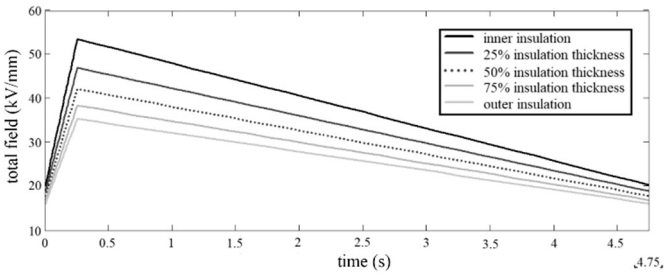

Fig. 9. Total electric field for the Cold Cable vs. time during the whole SSISP with $U_P=U_{P2,S,max}$=2.4 U_0 at 5 locations within the insulation. High set a_H,b_H

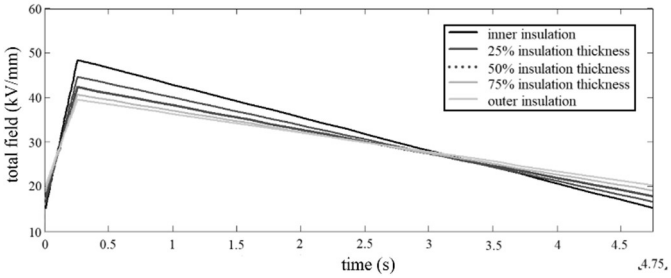

Fig. 10. Total electric field for the Hot Cable vs. time during the whole SSISP with $U_P=U_{P2,S,max}$=2.4 U_0 at 5 locations within the insulation. High set a_H,b_H

cumulated by the worst-case TOV vs. the SSISP depends also on waveform duration and is quantified preliminarily here via the loss-of-life fractions ΔLF listed in Table V. Table V clearly shows that the worst-case TOV always gives much higher loss-of-life fractions than the SSISP, included the most critical case: inner insulation, Cold Cable, a_L,b_L. This is even more true if – from the simulations done so far [2]-[9] - a possible upper limit of 200 ms is guessed for Δt_c instead of the order-of-magnitude value quoted in Table I, thereby emphasizing the role of the plateau. Thus, strictly-speaking SSISPs cannot encompass long TOVs as for cumulated aging effects.

In this respect, it is also worth pointing out what follows.

- The values of life fractions lost during the worst-case TOV in Table V are so low that their impact on cable reliability

TABLE III
COMPARISON BETWEEN THE HIGHEST TOTAL FIELD DUE TO THE TOV OF FIG. 1 AND THE HIGHEST TOTAL FIELD DUE TO THE SSISP, WITH a_L,b_L.

Voltage	Hot/Cold cable	Time interval	Duration (ms)	Max.field at inner insul.(kV/mm)	Max.field at outer insul.(kV/mm)
TOV	Cold	Δt_a	≈5	40.6 (at t_a)	26.2 (at t_a)
TOV	Cold	Δt_b	≈5	40.6 (at t_a)	26.2 (at t_a)
TOV	Cold	Δt_c	≈100	35.8(constant)	23.4(constant)
TOV	Hot	Δt_a	≈5	37.1 (at t_a)	28.7 (at t_a)
TOV	Hot	Δt_b	≈5	37.1 (at t_a)	28.7 (at t_a)
TOV	Hot	Δt_c	≈100	32.4(constant)	26.0(constant)
SSISP $2.15U_0$	Cold	T_S	4.75	48.9 (at T_1)	31.0 (at T_1)
SSISP $2.15U_0$	Hot	T_S	4.75	45.4 (at T_1)	33.5 (at T_1)
SSISP $2.4U_0$	Cold	T_S	4.75	54.8 (at T_1)	34.5 (at T_1)
SSISP $2.4U_0$	Hot	T_S	4.75	51.4 (at T_1)	37.0 (at T_1)

TABLE IV
COMPARISON BETWEEN THE HIGHEST TOTAL FIELD DUE TO THE TOV OF FIG. 1 AND THE HIGHEST TOTAL FIELD DUE TO THE SSISP, WITH a_H, b_H.

Voltage	Hot/Cold cable	Time interval	Duration (ms)	Max.field at inner insul.(kV/mm)	Max.field at outer insul.(kV/mm)
TOV	Cold	Δt_a	≈5	39.3 (at t_a)	27.1 (at t_a)
TOV	Cold	Δt_b	≈5	39.3 (at t_a)	27.1 (at t_a)
TOV	Cold	Δt_c	≈100	34.5 (constant)	24.3 (constant)
TOV	Hot	Δt_a	≈5	34.2 (at t_a)	31.3 (at t_a)
TOV	Hot	Δt_b	≈5	34.2 (at t_a)	31.3 (at t_a)
TOV	Hot	Δt_c	≈100	29.5(constant)	28.6(constant)
SSISP $2.15U_0$	Cold	T_S	4.75	47.6 (at T_1)	31.9 (at T_1)
SSISP $2.15U_0$	Hot	T_S	4.75	42.6 (at T_1)	36.2 (at T_1)
SSISP $2.4U_0$	Cold	T_S	4.75	53.5 (at T_1)	35.3 (at T_1)
SSISP $2.4U_0$	Hot	T_S	4.75	48.5 (at T_1)	39.6 (at T_1)

TABLE V
TOTAL LOSS-OF-LIFE FRACTIONS AT INNER INSULATION FOR THE TOV OF FIG. 1 IN COLD AND HOT CABLE CONDITIONS VS. TOTAL LOSS-OF-LIFE FRACTIONS AT INNER INSULATION FOR THE SSISP WITH a_L,b_L, a_M,b_M, AND a_H,b_H

a,b set ↓	waveshape ↓	Cold Cable		Hot Cable	
		loss-of-life fra.	Δ(%)	loss-of-life fra.	Δ(%)
a_L,b_L	SSISP	4.5×10^{-8}	-	2.2×10^{-8}	-
	TOV(Δt_c=100 ms)	1.0×10^{-7}	+122	3.7×10^{-8}	+68.2
	TOV(Δt_c=200 ms)	1.9×10^{-7}	+322	7.0×10^{-8}	+219
a_M,b_M	SSISP	1.2×10^{-8}	-	4.5×10^{-9}	-
	TOV(Δt_c=100 ms)	2.6×10^{-8}	+117	6.0×10^{-9}	+33.3
	TOV(Δt_c=200 ms)	4.8×10^{-8}	+300	1.1×10^{-8}	+144
a_H,b_H	SSISP	8.8×10^{-9}	-	3.0×10^{-9}	-
	TOV(Δt_c=100 ms)	1.8×10^{-8}	+105	3.8×10^{-9}	+26.7
	TOV(Δt_c=200 ms)	3.3×10^{-8}	+275	7.0×10^{-9}	+133

is expected to be negligible, when considering that the pole-to-ground faults which cause the worst-case TOV have a very low rate of occurrence. Indeed, according to [24] the typical failure rate of a submarine HVDC cable is ≈0.06 faults/year/100 km, involving 1 fault every ≈6 years in a 300 km-long line. Thus, based on [24] and Table V, the rate-of-occurrence of worst-case TOVs associated with faults in an HVDC line is so low that the relevant cumulated loss-of-life fraction throughout cable line service life can be neglected (see also [10]).

- Other service stresses – primarily rated voltage and the temperature set by loading cycles – consume a noteworthy fraction of cable insulation life, so that the life fraction left to SSISP and long TOVs is lower. Hence the true number of single SSISPs and long TOVs that HVDC extruded cable insulation can bear until failure is likely lower than the reciprocal of the total loss-of-life fractions in Table V, especially as the end of useful service life is approached.
- The calculations of life fractions lost are affected by uncertainties in the application of the followed approach to the high fields and the peculiar voltage waveforms associated with the long TOV and SSISP. In particular, the values in Table V are affected by the hypotheses made for loss-of-life fraction estimation, especially the use of the IPM life model (15) after [11]. In [10] it was shown that (15) can be used in the presence of both the DC and the AC component of field, since the IPM is employed also for Type Tests on EHV-AC extruded cables in Standard IEC 62067. However, its applicability might become uncertain at field values above Type-Test fields, since at these high fields insulation aging processes might change and more complex physical life models could be used [25],[26]. If this is the case, the estimates of total loss-of-life fractions reported in Table V for the worst-case TOV and for the SSISP might not be fully conservative.

In this respect, it should be assessed whether the maximum fields reached during the TOV – exceeding those during the LCTT, say, by 1÷6 kV/mm depending on the values of a,b and on Hot/Cold Cable conditions, see Tables IV-V in [10] – might overcome even the threshold for the onset of other damage processes, namely - in decreasing order of electric field level:

a) hot electron avalanches;
b) fast charge packets;
c) local space charge storage.

Hot electron avalanche processes can be neglected, since avalanches in crystalline PE occur at much higher electric fields than the maximum fields computed here for both the worst-case TOV (≈35÷40 kV/mm) and the SSISP (≈40÷55 kV/mm) [27].

As for local storage of space charge, experience shows that for well-designed and manufactured HVDC extruded cables local space charge effects should be a major concern neither at rated fields, nor at LCTT test fields [28]. They should not be a major problem even at the long TOV fields, unless these fields trigger particular dynamic phenomena, like fast charge packets.

Fast charge packets are clusters of both positive and negative charge carriers that cross the insulation all together and in a fast way, rather than through a step-by-step movement of single carriers injected at one or both electrodes. Fast charge packets have mobility values - in the range 10^{-10}-10^{-9} $m^2V^{-1}s^{-1}$ [29],[30] - that are unpredictable from typical packet theories involving traps, bulk insulation ions and high field electron/hole injection at electrodes [31]. Such packets bring large amounts of charge from one electrode to another, thereby creating hetero-charge layers that could cause early space-charge triggered failure. The onset of fast charge packets is due to complex phenomena related to electrode and dielectric materials, field and

temperature levels, additives or contaminants, and require the combination of high-enough field levels and long-enough application periods of such high electric fields [29],[30],[32].

For the sake of completeness, let us point out that, from a careful literature search, it cannot be excluded completely that the values of field (≈30-35 kV/mm, see Tables III-IV) and time duration (≈100 ms) of the plateau of the worst-case TOV of Fig. 1 may give rise to fast charge packets [29],[30] in certain cable designs. It should be highlighted that typically fast charge packets require first of all a constantly-applied DC field, and secondly of much larger value - of the order of 100 kV/mm - than those encountered not only during TOVs, but even during SSISP. However, the presence of non-cleaned nanofiller in a thin 1.5 mm specimen has been reported in [32] to reduce the threshold for packet generation from 100 kV/mm for a base, pure material, down to ≈40 kV/mm or less (thus compatible with the peak value of SSISP and TOV fields); the times required to cross such specimen (≈ hundreds ms) is much longer than the SSISP duration, but of the same order of magnitude of the TOV plateau (which has however fairly lower fields). On the other hand, full size cable insulation is much thicker than a 1.5 mm flat specimen, thus the chance that fast charge packets can be triggered under either SSISP or TOV fields is really remote even in cable insulation with non-cleaned nanofillers.

Of course, only dedicated experimental tests can assess high field effects - if any - on HVDC extruded insulation of TOV, SSISP and other transient voltage waveforms superimposed onto the DC voltage: a few tests with this goal have already started, see e.g. [33] as for TOVs and [34] as for SSISP.

V. Conclusions

The electric field calculations done in the framework of this study and reported in Part 1 paper have outlined that the maximum field during the worst-case long TOVs encountered in VSC HVDC cable systems - occurring at the inner surface of cable insulation - is higher than the maximum field at inner insulation during Type-Test loading cycles after CIGRÉ TB 496 in both Cold Cable (= no load) and Hot Cable (= full load) conditions. On the other hand, the field calculations carried out in the present Part 2 paper following the same computational approach as in Part 1 have revealed that the maximum fields during SSISP after TB 496 are higher than the maximum fields during the worst-case TOVs in both Cold and Hot Cable conditions, provided that a high-enough peak value of the switching impulse is taken: here, peak values ranging from 2.15 to 2.4 times the rated DC voltage have provided safety margins ranging from ≈17-19% to ≈26-29%, respectively, depending on the load level and on the values of electrical conductivity coefficients of the dielectric. Thus, as for the electrothermal stress, the SSISP could in principle encompass the long TOV from the viewpoint of the stressing effect on the extruded insulation of HVDC cables.

From computed electric fields, the values of total loss-of-life fraction at inner insulation during the SSISP have also been calculated, following an approach used only for cables under load cycling plus rated DC and AC voltage so far and applied for the first time to a transient voltage in Part 1 for the TOV and in the present Part 2 for the SSISP. The calculations (see Table V) show that the worst-case TOV always gives much higher loss-of-life fractions than the SSISP, included the most critical case: inner insulation, Cold Cable, lowest values of electrical conductivity coefficients of the dielectric. Thus, strictly-speaking SSISPs cannot encompass long TOVs as for cumulated aging effects. However, the loss of life computed for one single worst-case TOV is very small, thus it does not seem a major concern for the reliability of HVDC extruded cables.

Therefore, the main conclusions of this study at the present stage of the research can be summarized as follows.

1) The proposed method for a preliminary estimation of the effects of transient overvoltages on the reliability and life of HVDC extruded cables can be in fact applied for estimating the fractions of life lost during both TOVs and SSISP, as well as other possible superpositions of transient “AC-like” voltage over DC voltage. This makes the method generally applicable not only to TOVs and SSISP, but also to other voltage waveshapes;
2) According to the proposed method, the worst case TOV causes a much greater loss-of-life than the considered SSISP. Thus, strictly-speaking such SSISP cannot encompass long TOVs as for cumulated aging effects.
3) The loss-of-life estimated for worst case TOVs is very low. Thus, since the rate of occurrence of failure events leading to such TOV is very low, the overall loss-of-life cumulated by the cable in service due to worst case TOVs should be negligible and not of main concern.

For the sake of completeness, it is worth adding that from a careful literature search it cannot be totally excluded that the values of field and time duration during the long TOV are compatible with the onset of fast charge packets in certain cable designs. Such fast charge packets might accelerate the electro-thermal aging of cable insulation above the rate assumed in the life model used for loss of life estimation. If this were the case, the estimates of total loss-of-life fractions reported in Table V would not be fully conservative and tests other than Load Cycling Type Tests after TB 496 could assess quantitatively the potential threat of long TOVs.

However, again according to such literature search and as discussed in Section IV, this should not happen in a pure material, while the likelihood of such phenomenon in non-cleaned nanofillers would still be low for the thick insulation of full size cables. Thus, the chance that fast charge packets can be triggered in the presence of either SSISP or TOVs is remote, although only dedicated experimental tests can assess if such effects can be ruled out completely. The extensive analysis of such processes has not been completed at this stage of the research yet, but it might be useful in the future. On the other hand, this requires detailed information on insulation microstructure, insulation-semicon interfaces, etc., known exactly to manufacturers only.

As a last, but not least comment, accessory performance under long TOVs is an open topic that still needs to be investigated with specific studies focusing on accessory working conditions (field, temperature, interfaces, etc.).

VI. Acknowledgements

The authors acknowledge Dr. Massimo Marzinotto and Dr. Antonio Battaglia (TERNA SpA, Italy), with whom one author started since long time a fruitful discussion on long TOVs.

The authors also acknowledge CIGRÉ Joint Working Group B4/B1/C4.73 – of which one of the authors is member – from which he got the suggestion of studying long TOVs, of comparing long TOVs vs. SSISP, as well as the encouragement to submit here the related previously-unpublished results.

VII. References

[1] S. Mukherjee, M Saltzer, Y-J Häfner, and S Nyberg, "Cable overvoltage for MMC based VSC HVDC system: interaction with converters", Internat. Colloquium on H.V. Insulated Cables, New Delhi, India, 2017.

[2] T. Karmokar, M. Saltzer, S. Nyberg, S. Mukherjee, and P. Lundberg, "Evaluation of 320 kV extruded DC cable system for temporary overvoltages by testing with very long impulse waveform," CIGRÉ Session 2018 paper B1-123, Paris, August, 2018, pp. 1-11.

[3] M. Saltzer et al., "Overvoltages experienced by DC cables within an HVDC transmission system in a rigid bipolar configuration", Jicable'19, paper C5.1, Versailles (France), Jun. 23rd-27th 2019, pp. 1-6.

[4] F. B. Ajaei and R. Iravani, "Cable Surge Arrester Operation Due to Transient Overvoltages Under DC-Side Faults in the MMC HVDC Link," *IEEE Trans. Power Del.,* vol. 31, no. 3, pp. 1213–1222, Jun. 2016.

[5] H. Saad, P. Rault, and S. Dennetière, "Study on transient overvoltages in converter station of MMC-HVDC links," *Electr. Power Syst. Res*, vol. 160, pp. 397–403, Jul. 2018.

[6] S. Dennetière, H. Saad, A. Naud, P. Honda, "Transients on DC cables connected to VSC converters," in *9'th Int. Conf. on Insulated Power Cables* (*JICABLE),* Versailles, France, 2015.

[7] M. Goertz, S. Wenig, S. Beckler, C. Hirsching, M. Suriyah, T. Leibfried, "Analysis of Cable Overvoltages in Symmetrical Monopolar and Rigid Bipolar HVDC Configuration," *IEEE Trans. Power Deliv.,* vol. 35, no. 4, pp. 2097-2107, Dec. 2019.

[8] M. Goertz, S. Wenig, S. Beckler, C. Hirsching, M. Suriyah, T. Leibfried, "Overvoltage characteristics in symmetrical monopolar HB MMC-HVDC configuration comprising long cable systems," Proc. Int. Conf. Power Syst. Transients, Perpignan, France, Jun. 2019, pp. 1-6.

[9] Brochure CIGRÉ, *Surge and extended overvoltage testing of HVDC Cable Systems*, CIGRÉ Joint Working Group B4/B1/C4.73, 2021.

[10] G. Mazzanti, and B. Diban, *"*The effects of transient overvoltages on the reliability of HVDC Extruded Cables. Part 1: Long Temporary Overvoltages", accepted for publication in *IEEE Trans. Power Del.*, 2021.

[11] Brochure CIGRÉ 496, Recommendations for testing dc extruded cable systems for power transmission at a rated voltage up to 500 kV, prepared by CIGRÉ Working Group B1-32, Apr. 2012.

[12] High Voltage Direct Current (HVDC) Power Transmission Cables with Extruded Insulation and Their Accessories for Rated Voltages up to 320 kV for Land Applications - Test Methods and Requirements, IEC Standard 62895, 2017.

[13] IEC 60060-1, High-voltage test techniques. Part 1: General definitions and test requirements, Ed. 3, 2010.

[14] M.J.P. Jeroense, and P.H.F. Morshuis, "Electric fields in HVDC paper-insulated cables", *IEEE Trans. Dielectr. Electr. Insul.*, vol. 5, no. 2, pp. 225-236, Apr. 1998.

[15] G. Mazzanti, and M. Marzinotto, Extruded Cables for High Voltage Direct Current Transmission: Advances in Research and Development, IEEE Press Series on Power Engineering, Wiley-IEEE Press, 2013, ISBN 978-1-118-09666-6.

[16] R. N. Hampton, "Some of the considerations for materials operating under high-voltage, direct-current stresses," *IEEE Electr. Insul. Mag.,* vol. 24, no. 1, pp. 5–13, Jan./Feb. 2008.

[17] G. Mazzanti, "Life estimation of HVDC cables under the time-varying electrothermal stress associated with load cycles", *IEEE Trans. Power Del.*, vol. 30, no. 2, pp. 931 – 939, Apr. 2015.

[18] G. Mazzanti, "Including the calculation of transient electric field in the life estimation of HVDC Cables subjected to load cycles", *IEEE Electr. Insul. Mag.*, vol. 34, no. 3, pp. 27-37, May/Jun. 2018.

[19] B. Diban, and G. Mazzanti, "The effect of temperature and stress coefficients of electrical conductivity on the life of HVDC extruded cable insulation subjected to type test conditions," *IEEE Trans. Dielectr. Electr. Insul.*, vol. 27, no. 4, pp. 1295-1302, Aug. 2020.

[20] M.A. Miner, "Cumulative damage in fatigue", *J. Appl. Mechanics*, pp. A159-A163, Sep. 1945.

[21] G. Mazzanti, "Analysis of the combined effects of load cycling, thermal transients and electro-thermal stress on life expectancy of high-voltage ac cables", *IEEE Trans.Power Del.*, vol.22, no. 4, pp. 2000-2009, Oct. 2007.

[22] G. Mazzanti, "The combination of electro-thermal stress, load cycling and thermal transients and its effects on the life of high voltage ac cables", *IEEE Trans. Dielectr. Electr. Insul.*,vol.16,no.4,pp.1168-1179,Aug. 2009.

[23] G. J. Anders, and M. A. El-Kady, "Transient ratings of buried power cables. Part 1: Historical perspective and mathematical model," *IEEE Trans. Power Del.*, vol. 7, no. 4, pp. 1724–1734, Oct. 1992.

[24] Brochure CIGRÉ 815, Update of Service Experience of HV Underground and Submarine Cable Systems, prepared by CIGRÉ Working Group B1.57, 2020.

[25] G.C. Montanari, and G. Mazzanti, "From thermodynamic to phenomenological multistress models for insulating materials without or with evidence of threshold", J.Phys. D: Appl. Phys., vol.27, pp.1691-1702, 1994.

[26] G. Mazzanti, G. C. Montanari, and F. Civenni, "Model of inception and growth of damage from microvoids in polyethylene-based materials for HVDC Cables - Part 1: theoretical approach", IEEE Trans. Dielectr. Electr. Insul., pp. 1242-1254, vol. 14, n. 5, Oct. 2007

[27] H. Zeller, P. Pfluger, and J. Bernasconi, "High-mobility states and dielectric breakdown in polymeric dielectrics", *IEEE Trans. Electr. Insul.*, Vol. 19, pp. 200-204, 1984.

[28] E. Ildstad, J. Sletbak, B.R. Nyberg, and J.E.Lan, "Factors affecting the choice of insulation system for extruded HVDC power cables," CIGRÉ Session 2004, paper D1-203.

[29] A. See, L. A. Dissado, and J. C. Fothergill, "Electric field criteria for charge packet formation and movement in XLPE*", IEEE Trans. Dielectr. Electr. Insul.,* Vol. 8, pp. 859-866, 2001.

[30] D. Fabiani, G.C. Montanari, L. A. Dissado, C. Laurent, and G. Teyssedre, "Fast and slow charge packets in polymeric materials under DC stress", *IEEE Trans. Dielectr. Electr. Insul.*, Vol. 16, pp. 241-250, 2009.

[31] G.C. Montanari, G. Mazzanti, F. Palmieri, and B. Bertuzzi, "Mobility evaluation from space charge measurements performed by the pulsed electroacoustic technique", 6th Int. Conf. Prop. Appl. Diel. Mat. (IEEE ICPADM), vol. 1, pp. 38-41.

[32] G.C. Montanari, "Bringing an insulation to failure: the role of space charge", *IEEE Trans. Dielectr. Electr. Insul*., vol. 18, pp.339–364, 2011

[33] G. Mazzanti, P. Seri, B. Diban, and S. Stagni, "Preliminary experimental investigation of the effect of long temporary overvoltages on the reliability of HVDC extruded cables", IEEE Int. Conf. on Dielectr. (IEEE ICD 2020), pp. 49-52, Valencia, Spain, 6-31 Jul. 2020, Virtual Edition.

[34] G. Mazzanti, P. Seri, and B. Diban, "Preliminary experimental investigation of the effect of superimposed switching impulses on XLPE-insulated HVDC cables", submitted to IEEE Electr. Insul. Conf.2021.

Giovanni Mazzanti (M '04, SM '15, F '21) is associate professor of HV Engineering and Power Quality at the University of Bologna, Italy. His research interests are reliability and diagnostics of HV insulation, power quality, renewables, and human exposure to EMF. He is consultant to TERNA (the Italian TSO). He is author or coauthor of 290 published papers, and of the book Extruded Cables for HVDC Transmission: Advances in Research and Development, Wiley-IEEE Press, 2013. He is member of IEEE PES and DEIS, IEEE DEIS TC on "Smart grids" CIGRÉ JWG B4/B1/C4.73 on "Surge and extended overvoltage testing of HVDC Cable Systems", chair of the IEEE DEIS TC on "HVDC cable systems".

Bassel Diban (M'19) is currently a PhD student at the University of Bologna. His research interests are life modeling, reliability and diagnostics of HV insulation. He received bachelor's degree in electrical power engineering from Damascus University and later a master's degree in electrical energy engineering from the University of Bologna.